http://journal.uir.ac.id/index.php/JGEET

E-ISSN : 2541-5794
P-ISSN : 2503-216X

Journal of Geoscience,
Engineering, Environment, and Technology
Vol 11 No 3 2026

RESEARCH ARTICLE

2D and 3D Models of Rainfall-Induced Landslide-Prone Areas Using Electrical Resistivity Imaging (ERI) in Liku Sembilan, Central Bengkulu, Indonesia

Sefti Dewi Sari [1], Suhendra[1]*, Refrizon[1], Gina Soffia Novita[1], Halauddin[1], Hana Raihana[1], Yola Dwi Ramadhani[1]

[1] *Geophysics Study Program, Faculty of Mathematics and Natural Sciences, Bengkulu University, Bengkulu 38371, Indonesia*

* Corresponding author : suhendra@unib.ac.id
Tel.:+62 852-7938-5128
Received: Mar 1, 2026; Accepted: Jul 20, 2026.
DOI: 10.25299/jgeet.2026.11.3.27433

Abstract

Liku Sembilan, Central Bengkulu, is a landslide-prone area characterised by steep topography, intense weathering, and high annual rainfall. This study aims to identify the geometry and depth of the slip surface using integrated 2D and 3D Electrical Resistivity Imaging (ERI) to improve the characterisation of subsurface conditions associated with landslide occurrence. Data acquisition was conducted using the Wenner–Schlumberger array with 48 electrodes. The 2D survey was performed along a 94 m profile with 2 m electrode spacing, while the 3D survey covered approximately 1,750 m^2 using six parallel lines with 5 m line spacing and 10 m electrode spacing. Data were processed using Res2DInv and ERTLab-ViewLab3D. The inversion model produced an RMS error of 34.3% at the second iteration, which is considered acceptable given the complex topographic and geological conditions of the study area. The results reveal a low-resistivity zone (18–53 Ω·m) at a depth of approximately 5–10 m, interpreted as a water-saturated clay layer that serves as the main slip surface. The identified slip surface exhibits a curved geometry with a slope of 25–35°, indicating a rotational landslide mechanism. The integrated 2D and 3D ERI models provide a more comprehensive visualisation of the spatial continuity and geometry of the slip surface than a single-model approach. In addition, very low-resistivity zones (1–10 Ω · m) indicate areas of groundwater accumulation that may contribute to slope instability. These findings demonstrate the effectiveness of combined 2D and 3D ERI for landslide characterisation in tropical volcanic terrains and provide important information for slope-hazard mitigation and subsurface drainage planning.

Keywords: Electrical Resistivity Imaging (ERI), Landslide, Slip Surface, Liku Sembilan

1. Introduction

Landslides are one of the most common geomorphological disasters in Indonesia, particularly in areas with high rainfall intensity and sloping terrain (Lu et al., 2024). Bengkulu Province lies along the Bukit Barisan Mountain Range, which is highly vulnerable to landslides due to a combination of topographic, geological, and climatic conditions. One area particularly vulnerable to landslides is the Central Bengkulu–Kepahiang Highway, located in the Liku Sembilan area of Taba Penanjung Subdistrict, Central Bengkulu Regency. This area features steep slopes with gradients ranging from 15–45%, as well as high annual rainfall (averaging 4,003–5,439 mm/year), leading to frequent landslides that disrupt transportation and local economic activities (Alfarabi and Adhrianti, 2023; Natasya et al., 2022).

Rainfall is the primary trigger for landslides in Liku Sembilan. The infiltration of rainwater into the soil increases the water content and pore pressure, which in turn reduces the effective stress of the slope material. These conditions reduce soil shear strength and increase the potential for the formation of a slip surface in low-permeability layers, such as clay and silt (Jia et al., 2024; Zhang and Shen, 2024). From a geophysical perspective, an increase in soil moisture content in subsurface materials also decreases resistivity because pore fluid increases the material's electrical conductivity. Therefore, resistivity distribution can serve as an indicator of the presence of water-saturated zones and weak layers that contribute to slope-failure mechanisms (Chang et al., 2023; Hossain et al., 2023).

In recent years, landslides in the Liku Sembilan area have shown a strong correlation with periods of heavy rainfall. Recurring landslides at several points along the Central Bengkulu–Kepahiang route indicate that rainwater infiltration significantly triggers slope instability (BPBD, 2025). This phenomenon highlights the importance of understanding subsurface conditions, particularly the distribution of water-saturated zones and the presence of slip surfaces formed by rainwater accumulation.

Several previous studies on landslides in the Liku Sembilan area have identified a high landslide risk based on geological, geomorphological, and subsurface conditions (Abrar et al., 2024; Hadi et al., 2021; Natasya et al., 2022; Sugianto and Refrizon, 2021; Suhendra et al., 2018). However, most of these studies have primarily focused on mapping landslide potential and general slope characteristics. Information regarding the geometry of the slip surface, the distribution of water-saturated zones, and their relationship with variations in subsurface resistivity remains limited. Furthermore, subsurface interpretation is based on 2D cross-sections, so the spatial representation of the slip surface is not fully captured.

Recent international research indicates that the Electrical Resistivity Imaging (ERI) method is effective for

identifying slip planes, weathering zones, and subsurface water flow paths in landslide areas (Chumkhiao et al., 2025; Maleki et al., 2025; Sulaiman et al., 2023; Uwaezuoke et al., 2023). The integration of 2D and 3D resistivity models can improve the accuracy of slip-surface geometry interpretation and provide a better understanding of the relationship between hydrogeological conditions and slope stability than a single 2D approach. However, this approach has not been widely applied in tropical environments with high rainfall intensity, such as the Liku Sembilan area.

Given these conditions, there is a research gap in understanding the relationship between rainwater infiltration, the distribution of saturated zones, and the geometry of the slip surface in the Liku Sembilan area, as represented by a subsurface resistivity model. Previous research in Bengkulu has not integrated 2D and 3D ERI visualisations to spatially characterise slip surfaces or to evaluate their relationship with rainwater infiltration processes. Therefore, the novelty of this study lies in the integrated application of 2D and 3D ERI models to identify the presence, depth, and geometry of slip surfaces, and to interpret the relationship between saturated zones and subsurface resistivity responses on active tropical landslide slopes.

This study aims to identify the presence, depth, and structure of slip surfaces in the Liku Sembilan area using the ERI method, with results visualised in 2D and 3D models. The results of this study are expected to provide a more comprehensive understanding of the subsurface characteristics that control landslide occurrence and to serve as a scientific basis for disaster mitigation and risk reduction efforts in the region.

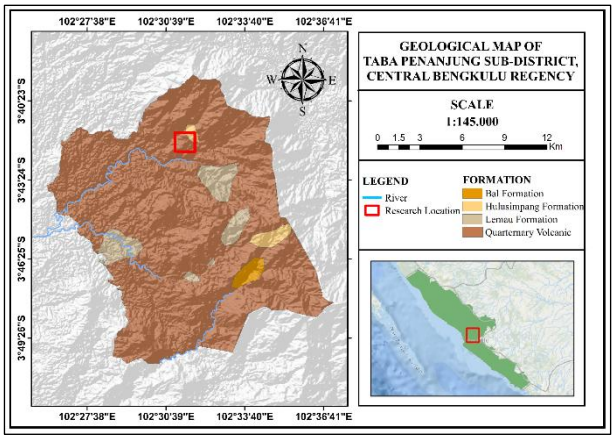

Fig. 1. Geological Map of Taba Penanjung Subdistrict, Central Bengkulu Regency.

2. Literature Review

2.1 Geological Conditions

The study area consists of hilly to mountainous terrain with elevations reaching approximately 1,020 meters above sea level and relatively steep slopes. These topographic conditions make the area prone to landslides, primarily due to a combination of slope gradients, rock weathering, and rainwater infiltration, which can increase the saturation of subsurface materials. Tectonically, the study area lies within the influence of the Sumatran Fault Zone, characterised by faults and rock fractures. These geological structures act as pathways for subsurface water flow, thereby accelerating weathering processes, increasing pore pressure, and reducing slope stability.

Based on the geological map of Taba Penanjung Subdistrict (**Figure 1**), the study area consists of the Hulusimpang Formation, the Bal Formation, the Lemau Formation, and Quaternary volcanic rocks (Gafoer et al., 2012). The Hulusimpang Formation is the oldest unit to have undergone hydrothermal alteration, resulting in a zone of relatively weathered, weaker rock than the fresh rock. These conditions can increase porosity and water storage capacity, thereby potentially creating a zone of slope instability (Harbowo et al., 2021; Zhuang et al., 2024).

The Bal Formation and the Lemau Formation consist of volcanic and sedimentary rocks with different permeability characteristics. Contrasts in physical properties between layers can lead to water accumulation at lithological contact boundaries and trigger an increase in pore water pressure, which contributes to the formation of slip planes (Wu et al., 2026). Meanwhile, the Quaternary volcanic rocks that dominate the study site have generally weathered to varying degrees, forming zones of more water-permeable material with reduced shear strength.

Differences in weathering levels, water content, and lithological characteristics result in variations in subsurface resistivity. Weathered and water-saturated materials generally exhibit low resistivity, whereas more compact and relatively dry rocks have higher resistivity. These resistivity contrasts form the basis for ERI interpretation to identify weak zones, water-saturation distribution, and indications of slip surfaces on slopes.

2.2 Slip Surface

The slip surface is a weak zone beneath the slope surface where soil or rock mass moves during a landslide. This zone typically develops in layers of low shear strength, such as clay, silt, or weathered material, that experience increased moisture content due to rainwater infiltration. Water accumulation in these layers can increase pore pressure and reduce effective stress, thereby reducing slope stability and triggering landslides (Bogaard and Greco, 2016; Zhuang et al., 2026). Slip surfaces often develop at the contact boundaries between layers that have different physical and hydraulic properties, particularly between weathered material and the relatively impermeable layer beneath it.

Based on their shape and movement mechanisms, slip surfaces can be classified into several main types: curved slip surfaces (rotational slip), planar or translational slip surfaces (translation slip), and compound slip surfaces (Hungr et al., 2014). Curved slip surfaces generally develop in relatively homogeneous soil materials of great thickness. In contrast, planar slip surfaces often form on layered slopes or in zones of discontinuity, such as rock strata and fracture surfaces. Meanwhile, compound slip surfaces are a combination of these two types and reflect more complex geological conditions (Azarafza et al., 2021; Huang, 2014). Understanding the types and characteristics of slip surfaces is a fundamental aspect of slope stability analysis and the assessment of landslide hazard potential.

In ERI investigations, the presence of slip surfaces is interpreted as zones of low resistivity associated with water-saturated clay layers or high-water-content weathered material. The resistivity contrast between water-saturated layers and more compact rock can be used to identify the presence and geometry of subsurface slip surfaces (Crawford et al., 2018). In tropical volcanic regions, slip surfaces often develop in the transition zone between water-saturated weathered material and more compact bedrock. These conditions produce resistivity contrasts

that are recognisable on ERI cross-sections as relatively sharp changes in resistivity or as continuous low-resistivity zones that follow the slope geometry (Caesario et al., 2024). Therefore, ERI interpretation is used not only to distinguish lithological units but also to identify the distribution of water saturation, the degree of weathering, and the geometry of the slip surface, all of which contribute to slope instability mechanisms.

3. Method

This study was conducted on the Central Bengkulu–Kepahiang Highway, specifically in the Liku Sembilan area of Central Bengkulu Regency, to determine the presence, depth, and structure of the slip surface layers using Electrical Resistivity Imaging (ERI). Subsurface investigation using the ERI method was carried out by measuring the potential difference of an area by injecting an electric current into the subsurface through current electrodes (Varamashvili et al., 2022). The ERI method has various electrode spacing configurations, such as Schlumberger, Wenner, and Dipole-dipole. In this study, the Wenner-Schlumberger configuration was selected because it offers good sensitivity in both vertical and horizontal directions and provides good resolution for 2D and 3D Modelling (Al-Zubedi and Abdulrazzaq, 2025). This configuration is also efficient for data collection and yields accurate results for identifying landslide-prone zones.

3.1 Wenner-Schlumberger Configuration

The operating principle of the Wenner-Schlumberger configuration can be explained using a constant-spacing system. As shown in (**Figure 2**), the scaling factor "n" is the ratio of the distance between the AM electrodes to the distance between the MN electrodes. If the distance between the potential electrodes MN is "a," then the distance between the current electrodes AB is "2na+a." Where I is the injection current, and V is the potential difference.

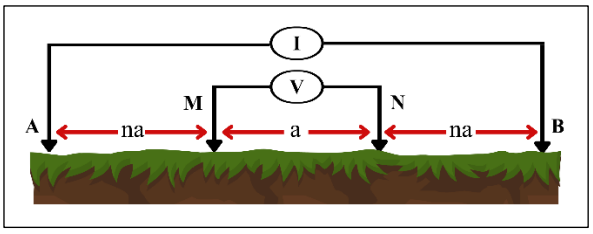

Fig 2. Wenner-Schlumberger Electrode Position.

The geometric factor (K) for the Wenner-Schlumberger configuration can be determined using equation (1) as follows:

$$K = n(n+1)\pi a \qquad (1)$$

Where a is the distance between electrodes M and N (Tongkeles et al., 2022).

3.2 Data Acquisition

Prior to data collection, a field survey must be conducted to determine the measurement design, geological conditions, and morphological characteristics of the study area (Hasan et al., 2022). Data collection was carried out in Liku Sembilan, Central Bengkulu, which was selected based on its history of landslides and slope conditions prone to mass movement. Data collection was performed using the Wenner-Schlumberger configuration of the ERI method on two profiles: a 2D profile and a 3D profile extending along the slope, as shown in (**Figure 3**). Data acquisition utilised the MAE X612-EM VHR Multi-Channel Resistivity Meter with 48 electrodes, programmed according to the measurement configuration. The 2D profile was 94 meters long with a 2-meter electrode spacing and was installed perpendicular to the slope. Meanwhile, the 3D survey was conducted using a grid pattern consisting of six parallel lines, with 5-meter spacing between lines and 10-meter spacing between electrodes, covering approximately 1,750 m^2. The difference in electrode spacing between the 2D and 3D lines was applied to align with the objectives of the subsurface investigation. The smaller electrode spacing on the 2D lines was used to achieve higher lateral and vertical resolution, making it more effective for identifying shallow zones, such as slip surfaces and weathered soil. Conversely, the larger electrode spacing on the 3D survey lines is used to achieve a wider area coverage and greater depth penetration, although with relatively lower resolution compared to the 2D survey lines. Based on the survey line length and configuration used, the estimated investigation depth for 2D survey lines ranges from ±15–20 meters, while 3D survey lines are estimated to reach depths of approximately ±18–25 meters, depending on subsurface conditions and the sensitivity of resistivity data.

The data obtained from the data collection include the distance from the current electrode to the centre point (AB/2), the distance from the potential electrode to the centre point (MN/2), the multiplication factor n, the injection current (I), the measured potential difference (ΔV), and the geometry factor (K). To ensure data quality, electrode contact resistance is monitored during the acquisition process. At points indicating poor ground contact, the electrodes were reinstalled and the soil around the electrodes was moistened to lower the contact resistance and reduce measurement noise. If inconsistent data or high error rates were found, the measurement was repeated until data meeting the acquisition quality standards were obtained.

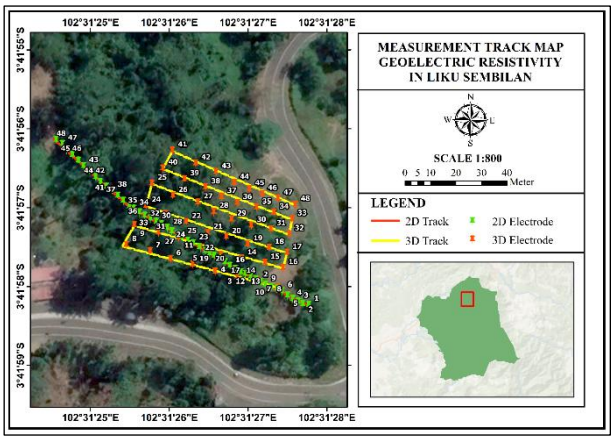

Fig. 3. Measurement Track Map Geoelectric Resistivity in Liku Sembilan.

3.3 Processing and Interpretation

2D data processing was performed using Res2Dinv software through several stages, including data quality checks, elimination of data with high error rates, and the inversion process. Topographic data for each electrode were obtained from position and elevation measurements using GPS during the field survey. This elevation data is then incorporated into the inversion process using the topographic correction feature in the Res2Dinv software so that the resulting resistivity model follows the slope

morphology and minimises distortion caused by topographic variations. The application of topographic correction is important for minimising model distortion arising from elevation variations in areas with steep topography (White et al., 2024).

The inversion process was performed using the least-squares inversion method with a smoothness-constraint approach to obtain a stable and representative subsurface resistivity model in a heterogeneous geological environment, including volcanic areas that have undergone intensive weathering and exhibit gradually varying resistivity (Ishola et al., 2014). The inversion is performed iteratively until a model is obtained that demonstrates a balance between a reduction in the misfit value and subsurface geological consistency (Doyoro and Chang, 2023).

3D data processing was performed using ERTlab software, integrating resistivity data with spatial coordinates, electrode positions, and topographic elevation. The integration of topographic data into 3D Modeling enables a more realistic reconstruction of subsurface geometry and reduces distortions caused by changes in terrain elevation. The inversion results are then visualised using ViewLab3D as horizontal and vertical volumes to analyse the distribution of resistivity anomalies at various depths.

Data interpretation is performed by considering the resistivity values of subsurface materials, local geological conditions, and slope morphological characteristics. The integrity of the results from the interpretation of 2D resistivity cross-sections and 3D resistivity models allows for the evaluation of the lateral and vertical continuity of resistivity anomalies, thereby enabling a more comprehensive interpretation of the geometry of the slip surface by considering the influence of structural and topographic factors on the distribution of anomalies.

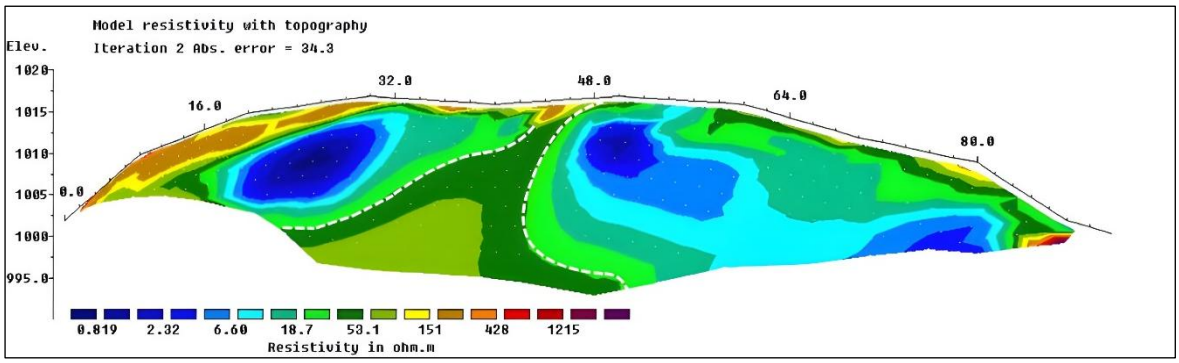

Fig. 4. 2D Modelling of the Research Area.

4. Result and Discussion

The results of the 2D resistivity data inversion using topographic data (**Figure 4**) show a distribution of resistivity values ranging from 0.819 Ω·m to 1215 Ω·m. This model yields an absolute error of 34.3% at the second iteration, which is relatively higher compared to several ERI studies in homogeneous environments, yet remains acceptable given the topographic complexity, lithological variations, and high water content distribution in the study area (Loke et al., 2013). The relatively high error value may be influenced by several factors, including the effects of topography on electrical current distribution, variations in electrode contact resistance, lithological heterogeneity and weathering levels, and the limitations of the inversion model in reconstructing geological conditions with contrasting resistivity changes.

The 2D model shows distinct lateral and vertical variations in resistivity values, reflecting differences in lithology and subsurface water saturation. The identified resistivity contrasts cannot be explained solely by changes in material type; they are also influenced by weathering levels, porosity, water content, and the electrical conductivity of the rock-forming minerals. Therefore, subsurface layer interpretation is based on a combination of resistivity values, geomorphological position, anomaly continuity, and local geological characteristics. In accordance with the interpretation in (**Table 1**), which shows low resistivity values (1–53 Ω·m) in blue-green as groundwater and clay, and medium to high ranges (200–1000 Ω·m) in yellow-red representing wet clay layers, weathered soil, and dry clay.

This interpretation is clearly evident in the 2D model (**Figure 4**), where the low-resistivity zone (18–53 Ω·m) extending to a shallow depth of approximately 5–10 meters is interpreted as a water-saturated clay layer. This interpretation is based on a combination of low resistivity values, the relatively continuous geometry of the layer, and its position beneath more resistive surface material. Geophysically, the low resistivity in this layer is likely influenced by the surface conductivity of clay minerals and increased electrolytic conduction due to water saturation (Cai et al., 2017). The combination of these two mechanisms produces a fairly distinct resistivity contrast with the surrounding layers and serves as a key indicator in identifying weak zones that may act as slip surfaces. The position of this zone follows the slope's topographic contours in a curved pattern, a characteristic feature of rotational-type slip surfaces. This interpretation is based not only on resistivity patterns but also on the geomorphological conditions of the slope, which indicate surface deformation and morphological changes consistent with mass movement processes (Masria et al., 2024).

Table 1. Interpretation of each layer in a 2D cross-section

Layer	Resistivity (**Ω**.m)
Aquifer	1-10
Clay	18-53
Wet clay	200-600
Weathering soil	200-800
Dry clay	800-1000
Igneous rock	>1215

The 3D model (Figure 5) provides a more comprehensive visualisation of the slip surface's spatial distribution from a three-dimensional perspective. In the 3D model, the slip surface is indicated by a blue-colored

zone, delineated by white dashed lines with a fairly steep slope following the slope topography at angles ranging from 25–35°, which is the critical angle range for landslides in residual soil and weathered soil (Huntley et al., 2019). The three-dimensional visualisation shows that this conductive zone extends laterally along the slope and forms a relatively continuous weak layer beneath the surface. The consistency in the location of the low-resistivity zone between the 2D and 3D models reinforces the interpretation that this layer constitutes the primary slip surface controlling the potential for mass movement.

The interpretation of slip surfaces in clay layers (18–53 **Ω**.m) is based on several geotechnical and geophysical considerations. Resistivity values in this range indicate that the clay material is in a wet to water-saturated state, possessing very weak mechanical properties, particularly low shear strength due to high water content. According to Crawford et al. (2018), water-saturated clay layers such as these often serve as locations for slip surfaces because they constitute zones with very low shear strength due to increased pore water pressure and reduced cohesion between clay particles. Suhendra et al. (2024) also identified clay layers with low resistivity values as weak slip planes using 2D and 3D ERT methods on the North Bengkulu–Lebong road section, supporting the findings of this study.

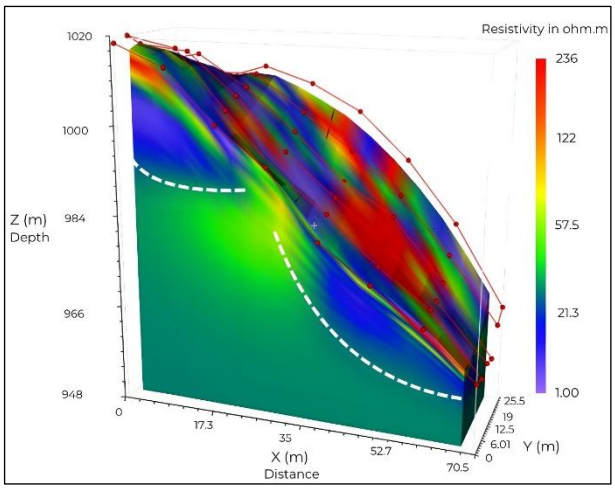

Fig. 5. 3D Modelling of the Research Area.

The effect of heavy rainfall on slope stability is evident from the presence of a zone of very low resistivity (1–10 **Ω**·m) above the slip surface. This zone indicates conditions with very high moisture content, approaching full saturation. Chambers et al. (2011) demonstrated that soil resistivity can decrease by 30–50% following intense rainfall due to increased water content in soil pores. The resistivity distribution pattern in the 2D model indicates that the low-resistivity zone is concentrated in the central part of the slope and lies directly above the clay layer interpreted as the slip surface. This condition suggests that infiltrated rainwater accumulates above the low-permeability layer, forming a water-saturated zone that can increase pore water pressure. Hydrogeologically, the clay layer acts as an aquitard that impedes vertical water movement and promotes lateral subsurface flow along the lithological contact (Bordoni et al., 2015). Nevertheless, the relationship between rainfall, water infiltration, and resistivity anomalies in this study remains interpretive because it is not supported by rainfall data, groundwater level measurements, or quantitative hydrogeological Modelling. Therefore, further research integrating rainfall data, groundwater levels, and temporal resistivity measurements is needed to obtain a more quantitative understanding.

Nevertheless, the interpretation obtained remains consistent with the climatic conditions of the Bengkulu region, which has high annual rainfall and landslide characteristics typical of tropical residual soils, in which rainwater infiltration is the primary factor controlling increases in pore water pressure and decreases in slope shear strength. The identification of slip surfaces using these 2D and 3D resistivity models is crucial for landslide disaster mitigation efforts. Understanding the position of the slip surface at a depth of approximately 5–10 meters, its curved geometry with a slope of about 25–35°, and the characteristics of water-saturated clay layers with resistivities (18–53 Ω·m) enables the planning of targeted mitigation strategies, such as installing horizontal drains at depths parallel to or slightly above the slip surface to accelerate groundwater discharge and reduce accumulated pore water pressure in the saturated zone, soil nailing or ground anchors that penetrate the thickness of the weak zone and are embedded in more competent material below the slip surface to increase the retaining force and slope safety factor, the use of retaining walls focused on critical areas showing the highest water accumulation based on the resistivity model, and counterweight berms placed at the toe of the slope to enhance slope stability.

5. Conclusion

The landslide disaster in Liku Sembilan, Central Bengkulu, was caused by a shallow slip surface. The slip surface was interpreted as a low-resistivity zone (18–53 Ω·m) at a depth of approximately 5–10 meters, representing a water-saturated clay layer. This zone forms a curved geometry with a slope of approximately 25–35°, indicating a rotational landslide mechanism. The identified resistivity contrast suggests that subsurface distribution is controlled by variations in lithology, weathering levels, and water saturation, which play a role in the formation of the slope's weak zone.

The integration of 2D and 3D ERI models provides a more comprehensive visualisation of the geometry of the slip surface and the distribution of subsurface weak zones in tropical volcanic environments. The findings of this study can serve as a basis for landslide disaster mitigation planning, particularly for the design of subsurface drainage systems and slope-stabilising retaining walls. However, the interpretations remain uncertain because geotechnical data, drilling, or hydrological monitoring do not yet support them. Therefore, further research with an integrated approach is needed to improve the reliability of interpretations and understanding of landslide mechanisms in the study area.

Acknowledgements

We want to thank the Learning and Student Information System (Simbelmawa) for funding this research through the PKM Technical Implementation Unit of Bengkulu University so that it could be carried out properly. We also extend our gratitude to the Geophysics Laboratory of Bengkulu University for providing the equipment (Multi-Channel Resistivity Meter MAE X612-EM, 48 Channels) and software (Res2Dinv, ERTlab, and ViewLab3D) throughout this research.

References

Abrar, C.B., Lubis, A.M., Fadli, D.I., Akbar, A.J., Samdara, R., 2024. Mapping Landslide Vulnerability using a Machine Learning Approach along the Taba Penanjung-Kepahiang Road, Bengkulu Province. Geoplanning 11, 43–56. https://doi.org/10.14710/geoplanning.11.1.43-56

Al-Zubedi, A.S., Abdulrazzaq, Z.T., 2025. The Resolution and Sensitivity Function of Electrode Arrays in 2D Resistivity Imaging Technique. Malaysian Journal of Science 44, 55–62. https://doi.org/10.22452/mjs.vol44no1.7

Alfarabi, A., Adhrianti, L., 2023. Strategi Komunikasi Resiko Bencana Bagi Upaya Penanggulangan Bencana Daerah (Studi Pemetaan Resiko Bencana Di Kabupaten Bengkulu Tengah). Ekspresi Dan Persepsi : Jurnal Ilmu Komunikasi 6, 146–158. https://doi.org/10.33822/jep.v6i1.5529

Azarafza, M., Akgün, H., Ghazifard, A., Asghari-Kaljahi, E., Rahnamarad, J., Derakhshani, R., 2021. Discontinuous rock slope stability analysis by limit equilibrium approaches – a review. International Journal of Digital Earth 14, 1918–1941. https://doi.org/10.1080/17538947.2021.1988163

Bogaard, T.A., Greco, R., 2016. Landslide hydrology: from hydrology to pore pressure. WIREs Water 3, 439–459. https://doi.org/10.1002/wat2.1126

Bordoni, M., Meisina, C., Valentino, R., Lu, N., Bittelli, M., Chersich, S., 2015. Hydrological factors affecting rainfall-induced shallow landslides: From the field monitoring to a simplified slope stability analysis. Engineering Geology 193, 19–37. https://doi.org/10.1016/j.enggeo.2015.04.006

BPBD, 2025. Pohon Tumbang dan Tanah Longsor di Liku Sembilan Taba Penanjung [WWW Document]. BPBD Kabupaten Bengkulu Teng. URL https://bpbd.bengkulutengahkab.go.id/postingan/detail_postingan/Pohon-Tumbang-dan-Tanah-Longsor-di-Liku-Sembilan-Taba-Penanjung (accessed 10.16.25).

Caesario, D., Aulia, B., Maiyudi, R., Khorniawan, W.B., Galih, A., Jayanti, R., 2024. An Understanding of Volcanic Deposits With Two-Dimensional Electrical Resistivity Imaging Survey at Talamau Mountain, West Pasaman , Indonesia. Sumatra J. Sumatra Journal of Disaster, Geography and Geography Education 8, 37–45.

Cai, J., Wei, W., Hu, X., Wood, D.A., 2017. Electrical conductivity models in saturated porous media: A review. Earth-Science Reviews 171, 419–433. https://doi.org/10.1016/j.earscirev.2017.06.013.

Chambers, J.E., Wilkinson, P.B., Kuras, O., Ford, J.R., Gunn, D.A., Meldrum, P.I., Pennington, C.V.L., Weller, A.L., Hobbs, P.R.N., Ogilvy, R.D., 2011. Three-dimensional geophysical anatomy of an active landslide in Lias Group mudrocks, Cleveland Basin, UK. Geomorphology 125, 472–484. https://doi.org/10.1016/j.geomorph.2010.09.017

Chang, P.Y., Doyoro, Y.G., Lin, D.J., Puntu, J.M., Amania, H.H., Kassie, L.N., 2023. Electrical resistivity imaging data for hydrogeological and geological hazard investigations in Taiwan. Data in Brief 49, 1–13. https://doi.org/10.1016/j.dib.2023.109377

Chumkhiao, R., Yindeesuk, S., Chao, K.C., Inazumi, S., 2025. Integrated geotechnical and electrical resistivity approaches for investigating rainfall-induced slope failure in a mountainous highway embankment. Transportation Geotechnics 55. https://doi.org/10.1016/j.trgeo.2025.101728

Crawford, Matthew, M., Bryson, Sebastian, L., 2018. Assessment of active landslides using field electrical measurements. Engineering Geology 233, 146–159. https://doi.org/10.1016/j.enggeo.2017.11.012

Doyoro, Y.G., Chang, P.Y., 2023. Importance of Estimating Measurement Noise in the Resistivity Imaging Inversion. European Association of Geoscientists & Engineers 2023, 1–5. https://doi.org/10.3997/2214-4609.202378040

Gafoer, S., Amin, T.C., Pardede, 2012. Geology of the Bengkulu Quadrangle, Sumatra. Department of Mines and Energy, Bandung.

Hadi, A.I., Refrizon, Farid, M., Harlianto, B., Sari, J.I., 2021. Landslide Potential Investigation for Disaster Risk Reduction in Central Bengkulu Regency, Bengkulu Province, Indonesia. Indonesian Journal of Geoscience 8, 313–328. https://doi.org/10.17014/ijog.8.3.313-328

Harbowo, D.G., Priadi, B., Julian, T., Amelia, R.N., Sihombing, D.J.P., Kencana, F.S., 2021. A preliminary study on the element abundance in the Hulusimpang Formation, Way Kalianda, Pesawaran, Lampung, Indonesia. IOP Conferences Series : Earth Environmental Science 882, 1–7. https://doi.org/10.1088/1755-1315/882/1/012078

Hasan, M.F.R., Salimah, A., Susilo, A., Rahmat, A., Nurtanto, M., Martina, N., 2022. Identification of Landslide Area Using Geoelectrical Resistivity Method as Disaster Mitigation Strategy. International Journal on Advance Science, Engineering and Information Technology 12, 1484–1490. https://doi.org/10.18517/ijaseit.12.4.14694

Hossain, A.T.M.S., Imam, M.H., Sayem, H.M., Khan, P.A., Haque, M.E., Khatun, M., Jafrin, S.J., Dutta, T., Mahmud, H., 2023. Electrical Resistivity Imaging for Characterising the Shallow Landslide Hazard Site at Kutupalong Rohingya Refugee Camps of Ukhiya, Cox's Bazar, Bangladesh. Earth Sciences 12, 223–243. https://doi.org/10.11648/j.earth.20231206.15

Huang, Y.H., 2014. Slope Stability Analysis by the Limit Equilibrium Method. American Society of Civil Engineers, Reston, VA. https://doi.org/10.1061/9780784412886

Hungr, O., Leroueil, S., Picarelli, L., 2014. The Varnes classification of landslide types, an update. Landslides 11, 167–194. https://doi.org/10.1007/s10346-013-0436-y

Huntley, D., Bobrowsky, P., Hendry, M., Macciotta, R., Elwood, D., Sattler, K., Best, M., Chambers, J., Meldrum, P., 2019. Application of multi-dimensional electrical resistivity tomography datasets to investigate a very slow-moving landslide near Ashcroft, British Columbia, Canada. Landslides 16, 1033–1042. https://doi.org/10.1007/s10346-019-01147-1

Ishola, K.S., Nawawi, M.N.M., Abdullah, K., Idriss, A., Sabri, A., Adiat, K.A., 2014. Assessment of the reliability of reproducing two-dimensional resistivity models using an image processing technique. SpringerPlus, 1–12.

Jia, J., Pei, X., Guo, X., Cui, S., Sun, P., Fan, H., Zhang, X., Gu, Q., 2024. Laboratory Model Tests on the Deformation and Failure of Terraced Loess Slopes Induced by Extreme Rainfall. Land 13, 1–22. https://doi.org/10.3390/land13101631

Loke, M.H., Chambers, J.E., Rucker, D.F., Kuras, O., Wilkinson, P.B., 2013. Recent developments in the direct-current geoelectrical imaging method. Journal of Applied Geophysics 95, 135–156. https://doi.org/10.1016/j.jappgeo.2013.02.017

Lu, W., Xiao, Z., Chen, Y., Sun, J., Chen, F., 2024. Spatiotemporal Characteristics and Rainfall Thresholds of Geological Landslide Disasters in ASEAN Countries. Atmosphere 15, 1–13. https://doi.org/10.3390/atmos15050599

Maleki, Z.R., Wilkinson, P., Chambers, J., Donohue, S., Holmes, J.L., Stirling, R., 2025. Geophysical Survey and Monitoring of Transportation Infrastructure Slopes (TISs): A Review. Geosciences 15, 1–51. https://doi.org/10.3390/geosciences15060220

Masria, A., Alshammari, T.O., Ghareeb, M., Seif, A.K., Abd-elmaboud, M.E., Ammar, A.I., 2024. 2D and 3D Modeling of resistivity and Chargeability to Identify the Type of Saturated Groundwater for Complex Sedimentary Facies. hydrology 11, 1–23. https://doi.org/10.3997/2214-4609.202378040

Natasya, I.D., Larang, M.P., Gatra Putri, E.G., Refrizon, R.R., 2022. Upaya Mitigasi Bencana Longsor Jalan Lintas Bengkulu-Kepahiang Berdasarkan Kecepatan Gelombang Geser (Vs). Newton-Maxwell Journal of Physics 3, 33–37. https://doi.org/10.33369/nmj.v3i1.21243

Sugianto, N., Refrizon, R., 2021. Struktur Kecepatan Gelombang Geser (Vs) di Daerah Rawan Gerakan Tanah (Longsor) Jalan Lintas Kabupaten Bengkulu Tengah-Kepahiang. Indonesian Journal of Applied Physics 11, 134–142. https://doi.org/10.13057/ijap.v11i2.41699

Suhendra, S., Sinaga, J.E.E., Fadli, D.I., Halauddin, H., Supiyati, S., 2024. 2D and 3D Modelling Electrical Resistivity Tomography (ERT) of Landslide Sliding and Weak Bedding Plane Along Mountain Road North Bengkulu-Lebong, Indonesia. Geosfera Indonesia 9, 29. https://doi.org/10.19184/geosi.v9i1.38065

Suhendra, Zul Bahrum, C., Sugianto, N., 2018. Geological condition at landslides potential area based on microtremor survey. ARPN Journal of Engineering Applied Sciences 13, 3007–3013.

Sulaiman, Noorzamzarina, Badros, A.S., Sulaiman, Nursufiah, Udin, W.S., Shafiee, N.S., Sulaiman, F.R., 2023. Landslide investigation using Electrical Resistivity Imaging (ERI) method at Kg. Chuchoh Puteri, Kuala Krai, Kelantan, Malaysia. BIO Web Conference 73, 1–8. https://doi.org/10.1051/bioconf/20237304003

Tongkeles, P.V., Suryantini, Pratama, A.B., 2022. The Application of Electrical Resistivity Tomography using Wenner-Schlumberger Arrays Configuration to Identify the Geological Structure in Kancah Warm Spring, West Java Indonesia. IOP Conference Series: Earth and Environmental Science 1047, 1–9. https://doi.org/10.1088/1755-1315/1047/1/012015

Uwaezuoke, Airen, C.C., John, O., 2023. Landslide Soil Failure Parameters Characterisation Using Geoelectrical Resistivity Methods in Uruagu , Nnewi , Anambra State , Nigeria. European Scientific Journal 19, 193–221. https://doi.org/10.19044/esj.2023.v19n12p193

Varamashvili, N.D., Kiria, J.K., Tarkhan-mouravi, A.G., Ghlonti, N.Y., 2022. The Possibility of Electroprospecting Methods in the Assessment of Subsurface Humidity and Groundwater Flow in a Landslide Area. Georgian Geophysical Society 25, 12–20. https://doi.org/10.48614/ggs2520224796

White, A., Boyd, J., Wilkinson, P., Unwin, H.E., Wookey, J., K, J.M., Binley, A., Chambers, J., 2024. Assessing the effect of topography on electrical resistivity measurements : insights from flood embankments. Geophysical Journal International 1117–1132. https://doi.org/10.1093/gji/ggae313

Wu, X., Xie, L., Wang, H., Fang, K., 2026. Effects of Pore Water Pressure on the Stability of Granular Slopes Under Simulated Rainfall. Geotechnical and Geological Engineering 44, 1–21. https://doi.org/10.1007/s10706-026-03630-8

Zhang, Q., Shen, D., 2024. Rainfall-Induced Landslides : Influencing , Modelling and Hazard Assessment. water 16, 1–5. https://doi.org/10.3390/w16233384

Zhuang, J., Wang, Z., Zhan, J., Zhu, Y., Chen, S., Chang, L., Dou, J., Hu, W., Guo, X., Peng, J., 2026. Evolution and failure mechanisms of water-induced landslide sliding zones. Engineering Geology 360, 108477. https://doi.org/10.1016/j.enggeo.2025.108477

Zhuang, Y., Hu, X., He, W., Shen, D., Zhu, Y., 2024. Stability Analysis of a Rocky Slope with a Weak Interbedded Layer under Rainfall Infiltration Conditions. water 16, 1–23. https://doi.org/10.3390/w16040604

© 2026 Journal of Geoscience, Engineering, Environment and Technology. All rights reserved. This is an open access article distributed under the terms of the CC BY-SA License (http://creativecommons.org/licenses/by-sa/4.0/).